



Biomechanical Investigation Between Rigid and Semirigid Posterolateral Fixation During Daily Activities: Geometrically Parametric Poroelastic Finite Element Analyses

OPEN ACCESS

Edited by:

Fabio Galbusera,
Galeazzi Orthopedic Institute (IRCCS),
Italy

Reviewed by:

Maxim Bashkuev,
Charité – Medical University of Berlin,
Germany

André P. G. Castro,
Universidade de Lisboa, Portugal

*Correspondence:

Chih-Hsiu Cheng
chcheng@mail.cgu.edu.tw

† These authors have contributed
equally to this work

Specialty section:

This article was submitted to
Biomechanics,
a section of the journal
Frontiers in Bioengineering and
Biotechnology

Received: 24 December 2020

Accepted: 02 March 2021

Published: 01 April 2021

Citation:

Nikkhoo M, Lu M-L, Chen W-C,
Fu C-J, Niu C-C, Lin Y-H and
Cheng C-H (2021) Biomechanical
Investigation Between Rigid and
Semirigid Posterolateral Fixation
During Daily Activities: Geometrically
Parametric Poroelastic Finite Element
Analyses.
Front. Bioeng. Biotechnol. 9:646079.
doi: 10.3389/fbioe.2021.646079

Mohammad Nikkhoo^{1†}, Meng-Ling Lu^{2,3†}, Wen-Chien Chen^{2,4}, Chen-Ju Fu^{2,5},
Chi-Chien Niu^{2,6}, Yang-Hua Lin⁷ and Chih-Hsiu Cheng^{2,7*}

¹ Department of Biomedical Engineering, Science and Research Branch, Islamic Azad University, Tehran, Iran, ² Bone and Joint Research Center, Chang Gung Memorial Hospital, Taoyuan, Taiwan, ³ Department of Orthopedic Surgery, Chang Gung Memorial Hospital, Kaohsiung, Taiwan, ⁴ Department of Orthopedic Surgery, Chang Gung Memorial Hospital, Taoyuan, Taiwan, ⁵ Division of Emergency and Critical Care Radiology, Chang Gung Memorial Hospital, Taoyuan, Taiwan, ⁶ Department of Orthopedic Surgery, Chang Gung Memorial Hospital, Taoyuan, Taiwan, ⁷ School of Physical Therapy and Graduate Institute of Rehabilitation Science, College of Medicine, Chang Gung University, Taoyuan, Taiwan

While spinal fusion using rigid rods remains the gold standard treatment modality for various lumbar degenerative conditions, its adverse effects, including accelerated adjacent segment disease (ASD), are well known. In order to better understand the performance of semirigid constructs using polyetheretherketone (PEEK) in fixation surgeries, the objective of this study was to analyze the biomechanical performance of PEEK versus Ti rods using a geometrically patient-specific poroelastic finite element (FE) analyses. Ten subject-specific preoperative models were developed, and the validity of the models was evaluated with previous studies. Furthermore, FE models of those lumbar spines were regenerated based on postoperation images for posterolateral fixation at the L4–L5 level. Biomechanical responses for instrumented and adjacent intervertebral discs (IVDs) were analyzed and compared subjected to static and cyclic loading. The preoperative model results were well comparable with previous FE studies. The PEEK construct demonstrated a slightly increased range of motion (ROM) at the instrumented level, but decreased ROM at adjacent levels, as compared with the Ti. However, no significant changes were detected during axial rotation. During cyclic loading, disc height loss, fluid loss, axial stress, and collagen fiber strain in the adjacent IVDs were higher for the Ti construct when compared with the intact and PEEK models. Increased ROM, experienced stress in AF, and fiber strain at adjacent levels were observed for the Ti rod group compared with the intact and PEEK rod group, which can indicate the risk of ASD for rigid fixation. Similar to the aforementioned pattern, disc height loss and fluid loss were significantly higher at adjacent levels in the Ti rod group

after cycling loading which alter the fluid–solid interaction of the adjacent IVDs. This phenomenon debilitates the damping quality, which results in disc disability in absorbing stress. Such finding may suggest the advantage of using a semirigid fixation system to decrease the chance of ASD.

Keywords: personalized modeling, finite element analysis, poroelastic, PEEK, titanium, spinal biomechanics, posterolateral fixation

INTRODUCTION

Degenerative lumbar diseases such as the spinal stenosis, lumbar instability, degenerative spondylolisthesis, and spondylolytic spondylolisthesis can cause clinical symptoms such as the low back pain (Serhan et al., 2011). Posterolateral fusion (PLF) and posterior lumbar interbody fusion (PLIF) techniques using rigid rods [i.e., pure titanium (Ti), Ti alloy, or cobalt-chrome (CoCr) rods] have been widely used in the treatment of degenerative lumbar disease (Schwab et al., 1995; De Iure et al., 2012; Campbell et al., 2017). However, the persistence of symptoms and the progression of degenerative disease were reported in some cases after PLF/PLIF, which is recognized as adjacent segment disease (ASD) (Rahm and Hall, 1996; Wang et al., 2017).

To minimize the incidence of ASD, several dynamic systems such as artificial discs and dynamic stabilization implants have therefore been introduced (Beatty, 2018) which can preserve intervertebral disc (IVD) motion and unload the stress on adjacent levels (Huang et al., 2016). However, the indications of these treatments are limited and they are not applicable to patients who still require fusion surgery. Subsequently, semirigid rods using polyetheretherketone (PEEK) were successfully used in fixation surgeries and good outcomes were reported (Highsmith et al., 2007). Nonetheless, some conflicting outcomes have also been reported in the literature when comparing PEEK rods against rigid ones after spinal fixation (Ormond et al., 2016).

While different clinical and biomechanical experimental studies were performed to evaluate the applicability of PEEK semirigid rods for non-fusion surgeries (Chou et al., 2015; Huang et al., 2016; Li et al., 2016; Selim et al., 2018), finite element (FE) modeling can be utilized, in parallel, as a practical tool for non-invasive investigations. Abundant FE studies have investigated the effect of different diseases/disorders (Schmidt et al., 2007b; Bashkuev et al., 2018; Ozkal et al., 2020) and relevant treatment modalities and techniques (Nikitovic et al., 2017; Rijsbergen et al., 2018; Zhang et al., 2018a; Heo et al., 2020) in lumbar spine. However, most of the available spinal FE models in the literature are limited to a single geometry which can cause uncertainty in the results and affect the reliability of FE model prediction for clinical application (Laville et al., 2009; Nikkhoo et al., 2019, 2020; Liu et al., 2020; Ozkal et al., 2020). Therefore, a workflow including procedural generation of patient-specific geometry for FE simulations can enhance our understanding of treatment results for adopting clinical approaches.

Choosing a proper formulation and assigning mechanical properties are essential to simulate the complex behavior of the spine. IVDs have a hydrostatic function by bearing and distributing mechanical loads, storing energy, and

restraining excessive motion in the spine. Since IVD is a non-homogeneous, well hydrated, and porous composite structure, various mathematical models (e.g., linear elastic, hyperelastic, viscoelastic, and poroelastic) were developed to simulate the biomechanics of the spine (Schmidt et al., 2013; Dreischarf et al., 2014). The intricate fluid–solid interactions in IVD, as a highly hydrated soft tissue, can be simulated by the poroelastic theory (Simon, 1992), and numerous studies used biphasic or multiphasic poroelastic FE models (Argoubi and Shirazi-Adl, 1996; Iatridis et al., 2003; Schmidt et al., 2010; Schroeder et al., 2010; Castro et al., 2014; Barthelemy et al., 2016; Castro and Alves, 2020) to mimic its time-dependent response. Hence, studying the biomechanical response of the spine during daily activities and assessment of the effect of damping characteristics (shock absorption mechanism) under cyclic loading could be beneficial when the objective is to investigate the spine biomechanics for spinal surgeries.

There remains a gap of knowledge in the detailed performance of semirigid constructs in spinal fixation surgeries to consider both the variation of anatomical geometries and the time-dependent response of the spine. Hence, the objective of this study was to comparatively analyze the biomechanical performance of PEEK versus Ti rods subjected to static and cyclic loading during daily activities using geometrically patient-specific poroelastic FE analyses.

MATERIALS AND METHODS

Patient-Specific Poroelastic FE Modeling

The geometries of the lumbosacral spine (L1–S1) were generated from lateral and anterior–posterior (AP) radiographs of 10 patients (age: 61.4 ± 8.1 years, BMI: 25.1 ± 1.7 kg/m², six females and four males) using a previously developed algorithm (Nikkhoo et al., 2020) (**Figure 1**). All patients presented with lumbar spine instability including single degenerative spondylolisthesis and spondylolytic spondylolisthesis in the lumbar region and underwent minimally invasive surgical procedures. All relevant clinical data were obtained from the data registry at Chang Gung Memorial Hospital, and a signed informed consent was acquired from all the participants prior to their enrolment in the clinical protocol, which was approved by the university research ethics committee.

Based on a previously validated FE model of the IVD (Nikkhoo et al., 2013a,b), a non-linear poroelastic FE model of the lumbosacral spine (L1–S1) was developed for 10 patients in relation to their preoperative (preop) geometries (**Figure 1**). Each FE model consists of six vertebrae (i.e., posterior bony elements

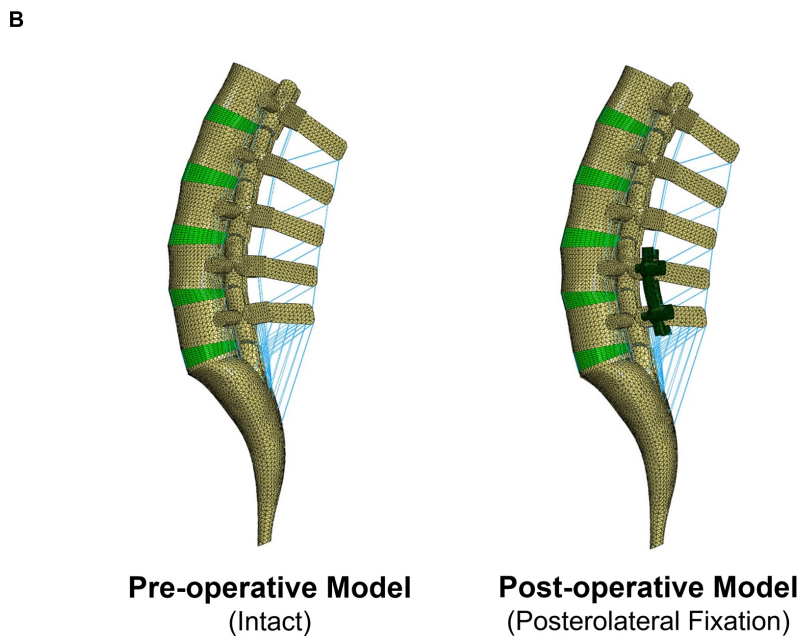
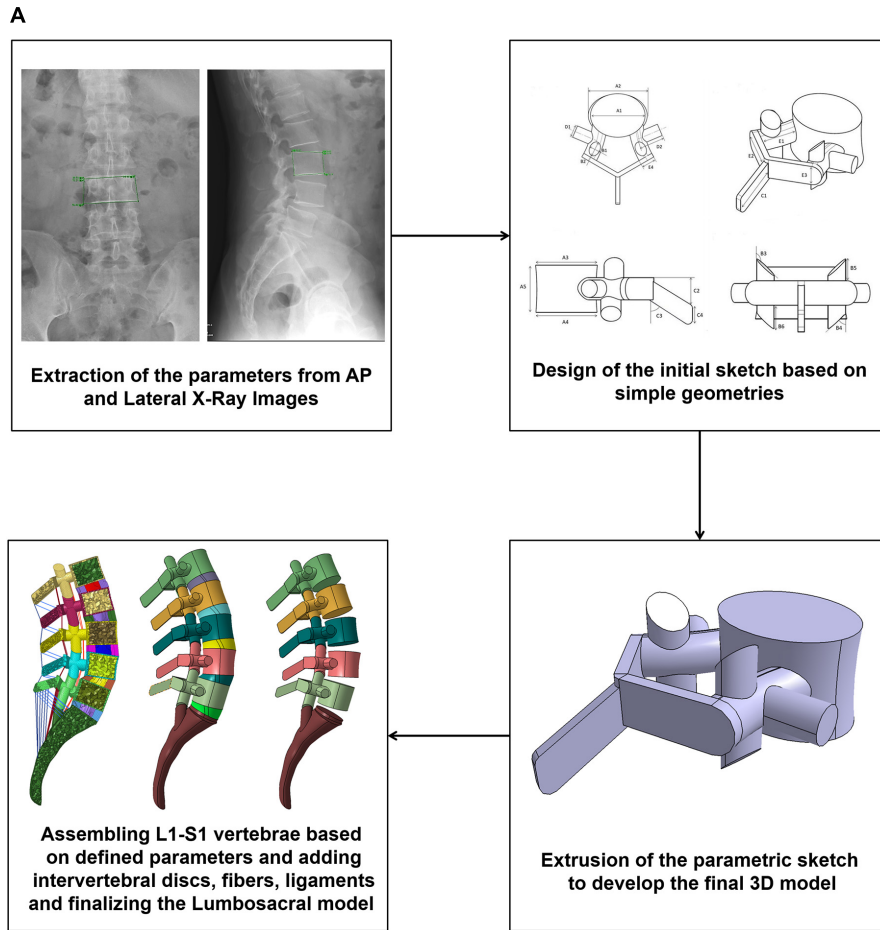


FIGURE 1 | (A) Procedure of personalized poroelastic finite element (FE) modeling of the lumbosacral spine and **(B)** preoperative (intact) and postoperative (posterolateral fixation) FE models.

and vertebral bodies including cancellous and cortical bones), five IVDs and 10 endplates (i.e., L1–L2, L2–L3, L3–L4, L4–L5, L5–S1), and seven ligaments [i.e., anterior longitudinal ligament (ALL), posterior longitudinal ligament (PLL), ligamentum flavum (LF), transverse ligament (TL), capsular ligament (CL), interspinous ligament (ISL), and supraspinous ligament (SSL)], as well as five pairs of facet joints. The IVDs were represented by a reinforced composite material including the annulus fibrosus (AF), ground substance, nucleus pulposus (NP), and AF collagen fibers.

The non-linear drained solid phase of the AF and NP was simulated based on the Mooney–Rivlin hyperelastic theory in alignment with the literature (Schmidt et al., 2007a; El-Rich et al., 2009) (**Table 1**). Poroelasticity was considered for vertebral bodies, endplates, and IVDs in the FE model. Permeability values were considered dependent on void ratio (**Table 1**) (Argoubi and Shirazi-Adl, 1996; Ferguson et al., 2004) as follows:

$$k = k_0 \left[\frac{e(1 + e_0)}{e_0(1 + e)} \right]^2 \exp \left[M \left(\frac{1 + e}{1 + e_0} - 1 \right) \right] \quad (1)$$

Where k_0 is the initial permeability and e is defined as follows:

$$e = \frac{\emptyset_f}{1 - \emptyset_f} \quad (2)$$

Where \emptyset_f is the porosity of the tissue which varies with tissue deformation. The six concentric reinforced fiber layers with an orientation of $\pm 35^\circ$ within a distance of 1 mm were embedded in the AF ground substance (Naserkhaki et al., 2016). A constant boundary pore pressure of 0.25 MPa was imposed on all external surfaces of the IVDs to mimic the swelling phenomenon (Schmidt et al., 2010; Galbusera et al., 2011a). Ligaments were modeled using non-linear truss elements which could be activated only in tension (**Figure 2**) (Shirazi-Adl et al., 1986a; Pintar et al., 1992). The ligaments were attached at fixed points in a primary standard anatomy-based geometrical lumbosacral spine model, and their length could be updated according to the measured parameters of the bony parts for different individuals.

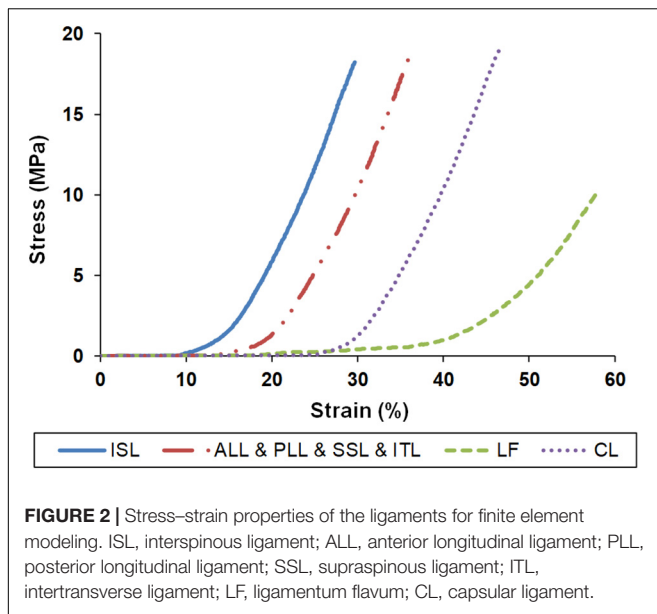
The mechanical properties of the other tissues were adopted based on previous studies (Shirazi-Adl et al., 1986b; Goto et al., 2003; Schmidt et al., 2007a) (**Table 1**). To simulate the articulation of the facet joints, a surface-to-surface contact rule for both tangential and normal directions was applied to model within a gap length of 0.5 mm (Naserkhaki et al., 2016; Naserkhaki and El-Rich, 2017). The meshing sensitivity analyses were performed, and the FE models were evaluated using a total of 186,325 elements for all the models.

The validity of the IVD time-dependent response was previously validated based on the achieved results from a motion

TABLE 1 | Mechanical properties of the patient-specific poroelastic finite element model.

Spinal component	Material behavior	Mechanical properties	References
Cortical bone	Linear poroelastic	$E = 12,000$ MPa, $\nu = 0.3$, $k_0 = 1 \times 10^{-20}$ (m ⁴ /N s), $e = 0.02$	Argoubi and Shirazi-Adl, 1996; Goto et al., 2003; Ferguson et al., 2004; Schmidt et al., 2010; Galbusera et al., 2011b; Park et al., 2013
Cancellous bone	Linear poroelastic	$E = 200$ MPa, $\nu = 0.25$, $k_0 = 1 \times 10^{-13}$ (m ⁴ /N s), $e = 0.4$	Argoubi and Shirazi-Adl, 1996; Ferguson et al., 2004; Schmidt et al., 2007a, 2010; Galbusera et al., 2011b; Shih et al., 2013
Endplate	Linear poroelastic	$E = 5$ MPa, $\nu = 0.1$, $k_0 = 7.5 \times 10^{-15}$ (m ⁴ /N s), $e = 4$	Argoubi and Shirazi-Adl, 1996; Goto et al., 2003; Ferguson et al., 2004; Schmidt et al., 2007a, 2010; Galbusera et al., 2011b
Annulus fibrosus ground	Incompressible poro-hyperelastic (Mooney–Rivlin)	$C10 = 0.18$, $C01 = 0.045$, $k_0 = 3 \times 10^{-16}$ (m ⁴ /N s), $e = 2.33$	Argoubi and Shirazi-Adl, 1996; Ferguson et al., 2004; El-Rich et al., 2009; Schmidt et al., 2010; Galbusera et al., 2011b
Nucleus pulposus	Incompressible poro-hyperelastic (Mooney–Rivlin)	$C10 = 0.12$, $C01 = 0.030$, $k_0 = 7.5 \times 10^{-16}$ (m ⁴ /N s), $e = 4$	Argoubi and Shirazi-Adl, 1996; Ferguson et al., 2004; Schmidt et al., 2007a, 2010; Galbusera et al., 2011b
Collagen fibers	Non-linear elastic	Stiffness increasing from the inner to the outer layer	Shirazi-Adl et al., 1986b; Schmidt et al., 2006
ALL, PLL, LF, ISL, SSL, ITL, CL	Non-linear elastic	Non-linear curves in Figure 2	Shirazi-Adl et al., 1986a; Pintar et al., 1992
Pedicle screws	Elastic	$E = 110,000$ MPa, $\nu = 0.3$	Zhang et al., 2018b
Rigid rod (Ti)	Elastic	$E = 110,000$ MPa, $\nu = 0.3$	Zhang et al., 2018b
Semirigid rod (PEEK)	Elastic	$E = 3,500$ MPa, $\nu = 0.3$	Zhang et al., 2018b

ALL, anterior longitudinal ligament; PLL, posterior longitudinal ligament; LF, ligamentum flavum; ISL, interspinous ligament; SSL, supraspinous ligament; ITL, intertransverse ligament; CL, capsular ligament.



segment subjected to short-term creep, long-term creep, and a daily cycle (Nikkhoo et al., 2013a; Ghobadiha et al., 2019). To evaluate the validity of the preop lumbar spine FE models, a combined loading scenario (i.e., the combination of the compressive forces and bending moments; **Table 2**) (Dreischarf et al., 2011, 2014) was applied to the models and the results of range of motion (ROM), intradiscal pressure (IDP), and facet joint forces (FJF) were compared with previous numerical studies from eight well-established FE models of the lumbar spine (Dreischarf et al., 2014). To apply the physiological compression loads, the follower load technique (Patwardhan et al., 1999; Shirazi-Adl and Parnianpour, 2000; Dreischarf et al., 2014) was used as described in **Table 2**. The rotational moments were applied to the superior surface of L1, and Dirichlet boundary conditions were considered at the sacral region to inhibit any displacement/rotation in all degrees of freedom.

Patient-Specific Posterolateral Fixation FE Modeling

Biomechanical investigation between rigid and semirigid posterolateral fixation during daily activities was selected as the application for this validated parametric poroelastic model. For this purpose, postoperative (postop) FE models of the same patients were regenerated and developed based on postop images. Posterolateral fixation surgery at the L4–L5 level was mimicked in the FE models by simulating a wide laminectomy and removing the PLL and LF while preserving the IVD and spinous process. A posterior bilateral pedicle screw fixation construct was then implemented based on measurements from the postop images. The screws and rods were considered as linear elastic based on reported data in the literature (Zhang et al., 2018b) (**Table 1**). Tie contact condition was used to constrain equal translational and rotational motions for attached surfaces between the vertebrae, screws, and rods for mimicking the permanent fusion. For each patient, the simulations were performed using corresponding

materials for Ti and PEEK (**Table 1**) with the relevant postop model (**Figure 1B**). Following an 8-h preconditioning resting period under the constant compressive load of 200 N (Galbusera et al., 2011a), a 16-h cyclic compressive loading of 500–1,000 N (40 and 20 min, respectively) was applied to the postop FE models. The cyclic axial compressive loading was simulated by the follower load technique (Patwardhan et al., 1999; Shirazi-Adl and Parnianpour, 2000; Dreischarf et al., 2014) using connector elements. Different rotational movements (i.e., flexion, extension, right and left lateral bending, and right and left axial rotation) were superimposed using 10 N m moment before and after cyclic loading (i.e., points 1 and 2 in **Figure 3**) to model the rotational motions in the morning and evening. The rotational moments were linearly applied and removed in 10 s (i.e., 5 s for loading and 5 s for unloading), and only one motion was evaluated in each diurnal loading simulation. The rotational moments were applied to the superior surface of L1, and Dirichlet boundary conditions were considered at the sacral region. Biomechanical responses including motion patterns, IVD height loss, fluid loss, experienced stress in AF, and collagen fiber strain were analyzed before and after cyclic loading under the same loading and boundary conditions.

Statistical Analyses on the Results of Different FE Models

The simulation results of the motion patterns (i.e., ROM), disc height loss, fluid loss, experienced stress in AF, and collagen fiber strain were all compared among the rigid and semirigid models. As the data were not normally distributed, the non-parametric Friedman with Nemenyi *post hoc* tests were conducted to determine the differences of the calculated results. The *p* values less than 0.05 were considered as significant statistical differences.

RESULTS

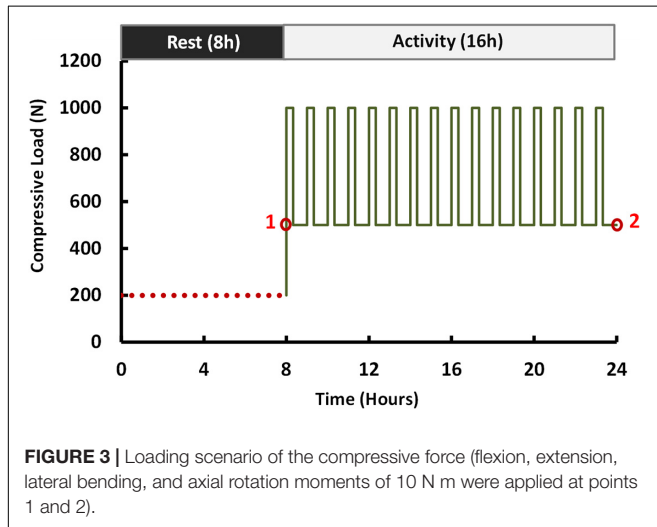
The numerical precisions for the FE models were verified using mesh sensitivity analyses. The intersegmental ROMs for the preop models were consistent with previous numerical data from the literature (**Figure 4**). Besides, the calculated IDP (**Figure 5**) and FJF (**Figure 6**) fell within a comparable range to previous studies in different directions.

Compared with preop FE models, the ROMs at the instrumented level were significantly decreased for both Ti (averagely decreased to 4.01° in flexion, 2.62° in extension, 2.45° in lateral bending, and 1.18° in axial rotation) and PEEK (averagely decreased to 2.95° in flexion, 1.87° in extension, 1.92° in lateral bending, and 1.06° in axial rotation) fixation systems (**Figure 7A**). However, the calculated ROMs at the instrumented level were higher for the PEEK construct in flexion, extension, and lateral bending (**Figure 7A**). The ROMs at the adjacent levels were significantly increased for Ti rods compared with the intact models in flexion, extension, and lateral bending (**Figures 7B,C**). Nonetheless, no significant changes were detected between the ROM of the adjacent IVDs for the intact and PEEK construct FE models (**Figures 7B,C**).

TABLE 2 | Combined loading conditions for simulation of lumbar spine in different movements.

Direction	Compressive load* (N)	Moment (N m)	References
Flexion	1,175	7.5	Rohlmann et al., 2009; Dreischarf et al., 2014
Extension	500	7.5	Rohlmann et al., 2009; Dreischarf et al., 2014
Lateral bending	700	7.8	Dreischarf et al., 2012, 2014
Axial rotation	720	5.5	Dreischarf et al., 2011, 2014

*The follower load technique (Patwardhan et al., 1999; Shirazi-Adl and Parnianpour, 2000; Dreischarf et al., 2014) was used to simulate the compressive loading.



During cyclic loading, the disc height averagely decreased by 6.58, 6.13, and 5.79% at L3–L4, L4–L5, and L5–S1, respectively, in the intact FE models. In postop models, increased disc height loss and fluid loss in adjacent levels were observed for Ti fixation system models compared with the intact ones (Figure 8). Moreover, disc height loss and fluid loss in the adjacent IVDs were significantly higher for the Ti construct when compared with the PEEK models (Figure 8). The axial stress and collagen fiber strain in AF significantly increased in adjacent levels for posterolateral fixation models (Figures 9, 10) in flexion and extension. However, the axial stress and collagen fiber strain in adjacent IVDs were higher for the Ti construct when compared with the PEEK models (Figures 9, 10). The variations of the increased stress and fiber strain in adjacent levels were minimal and not significant for lateral bending and axial rotation, respectively, after applying the cyclic loading (Figures 9, 10).

DISCUSSION

The rigid instrumented PLF and PLIF have been the gold standard treatment techniques for spinal stenosis, disc degeneration, and spondylolisthesis. Conversely, numerous studies have demonstrated unwanted side effects of the rigid PLF/PLIF, including pseudarthrosis, loss of motion, back pain, and ASD (Rahm and Hall, 1996; Wang et al., 2017). It was reported that using an interbody device can enhance the postop biomechanical stability and increase the fusion rate

(Lidar et al., 2005; Aygün et al., 2014; Lee et al., 2014; Campbell et al., 2017). However, implanting the interbody device may increase the segmental rigidity which could result in increasing the mechanical stress to the adjacent segments (Chiang et al., 2006; Sudo et al., 2006). A less rigid stabilization system can theoretically preserve part of rotational motion in instrumented level and unload the extra exposed stress on adjacent levels (Lee et al., 2014; Huang et al., 2016). Therefore, a quantitative study to analyze the biomechanical behavior of the lumbar spine in response to PLF surgery using rigid versus semirigid rods may be beneficial for clinicians. Spinal fixation construct is the most essential part of the fusion approach, and the current study therefore aimed to investigate the fixation itself. For this purpose, the posterolateral fixation was utilized for simulating the postop models with Ti and PEEK rods, and the bone graft fusion between the transverse processes was neglected, which is a common simplification in the literature (Goto et al., 2003; Gornet et al., 2011; Jin et al., 2012; Jahng et al., 2013).

The current study employed a geometrically patient-specific poroelastic FE modeling technique to evaluate the intersegmental motions and load sharing of the lumbar spine by developing pre- and postop simulations. The time-dependent responses of the FE model subjected to cyclic loading were investigated in this study by considering the poroelastic theory for vertebra, IVDs, and endplates which was mostly ignored in previous relevant studies (Jin et al., 2012; Jahng et al., 2013; Guo et al., 2019). Considering a time-dependent model by calculating the interactions of disc solid structures and interstitial fluid can determine IVD endurance to cyclic loadings (Galbusera et al., 2011b; Castro et al., 2018). Therefore, this study provided the calculated disc height loss, fluid loss, altered stress, and strain in the AF region which can better quantify the effect of rigid and semirigid posterolateral fixation surgery on biomechanical response of the lumbar spine.

Moreover, we used a parametric subject-specific FE model which can be regenerated for different patients based on simple lateral and AP X-ray images. Hence, we repeated the simulations for 10 patients (in total, 30 pre- and postop FE models) to consider interanatomical variability to investigate the influence of posterolateral fixation surgery using rigid and semirigid rods. Repeating the calculations for different patients and considering the influences of the geometry (anatomical parameters such as vertebra dimensions, disc height, lordosis angle, etc.) can better evaluate if the observed differences in the results for rigid versus semirigid posterolateral fixation systems are significant or not. Previous FE models in the literature are constrained to unique geometry, typically based on one subject. The intrinsic geometric

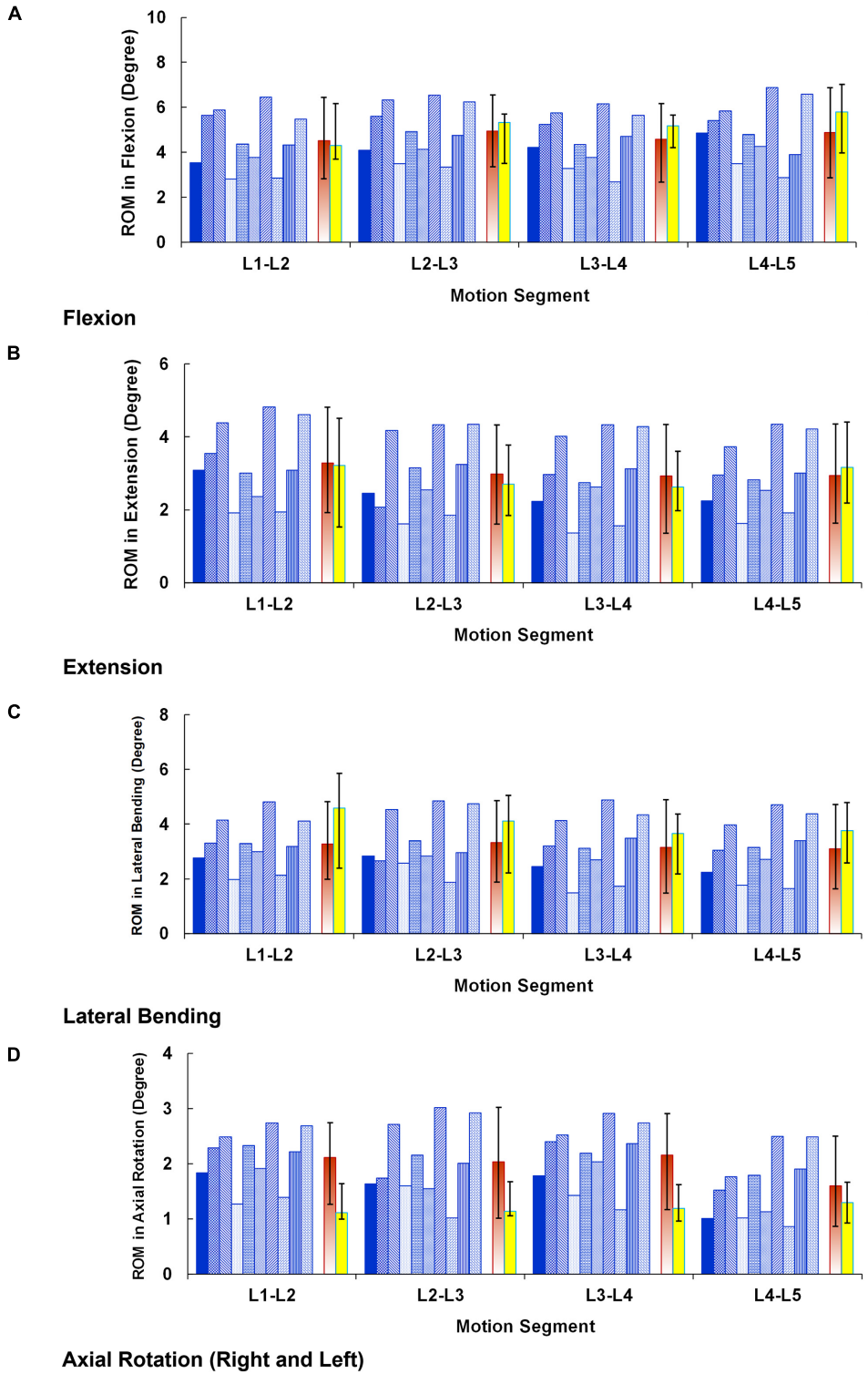
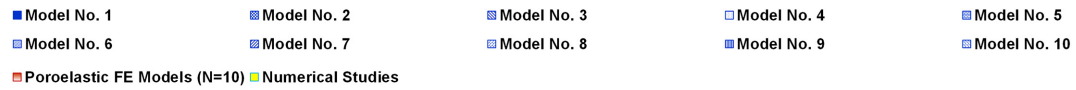


FIGURE 4 | Intersegmental range of motions (ROMs) for preoperative FE models compared with the numerical studies (Dreischarf et al., 2014) in **(A)** flexion, **(B)** extension, **(C)** lateral bending, and **(D)** axial rotation. The reported ROMs in lateral bending and axial rotation are the average in the left and right directions. The error bars indicate the ranges of the results.

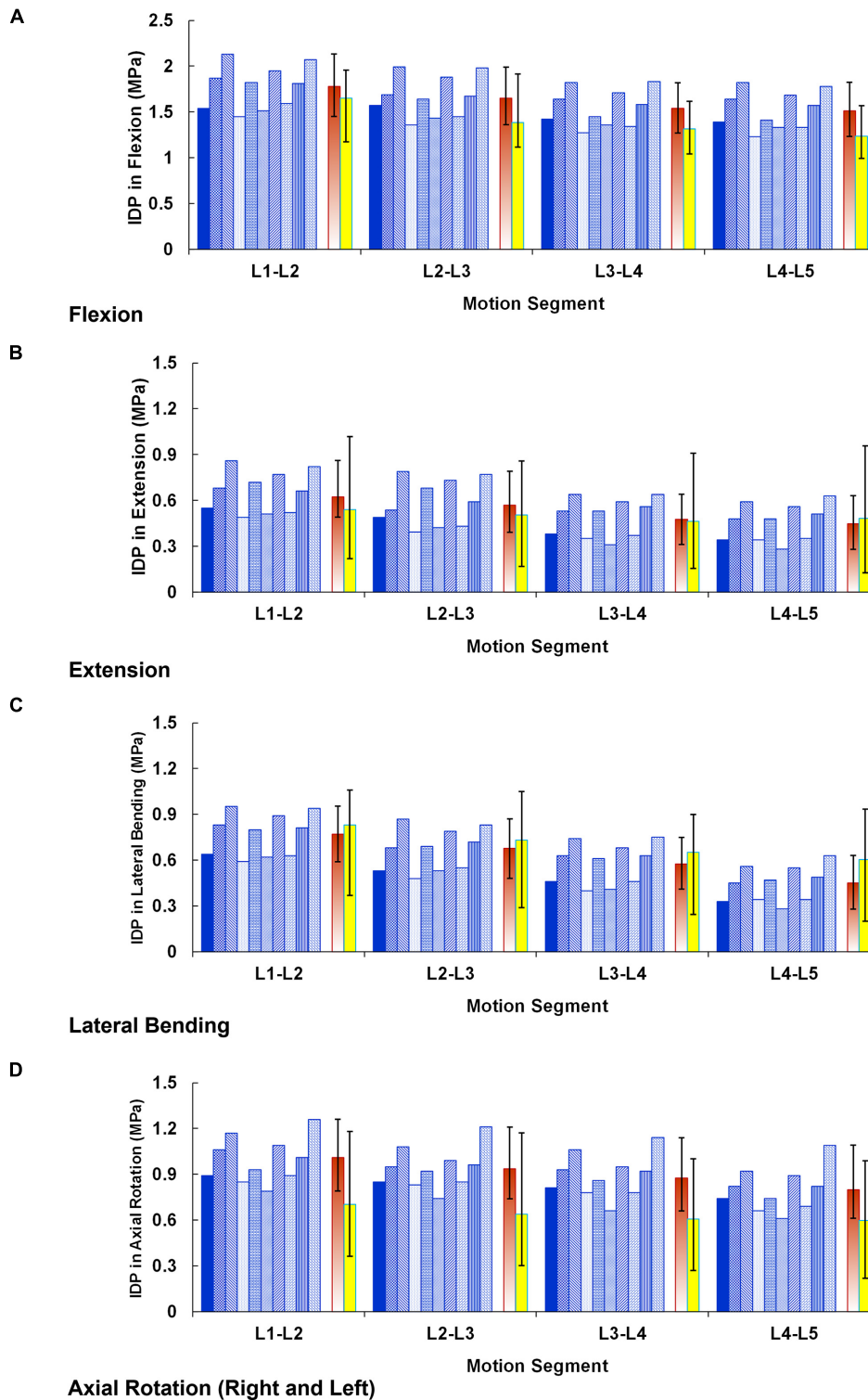
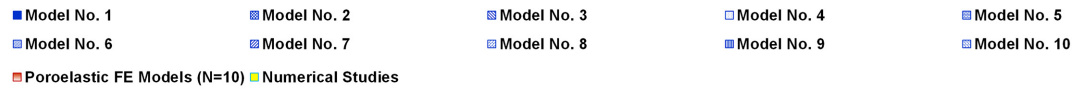
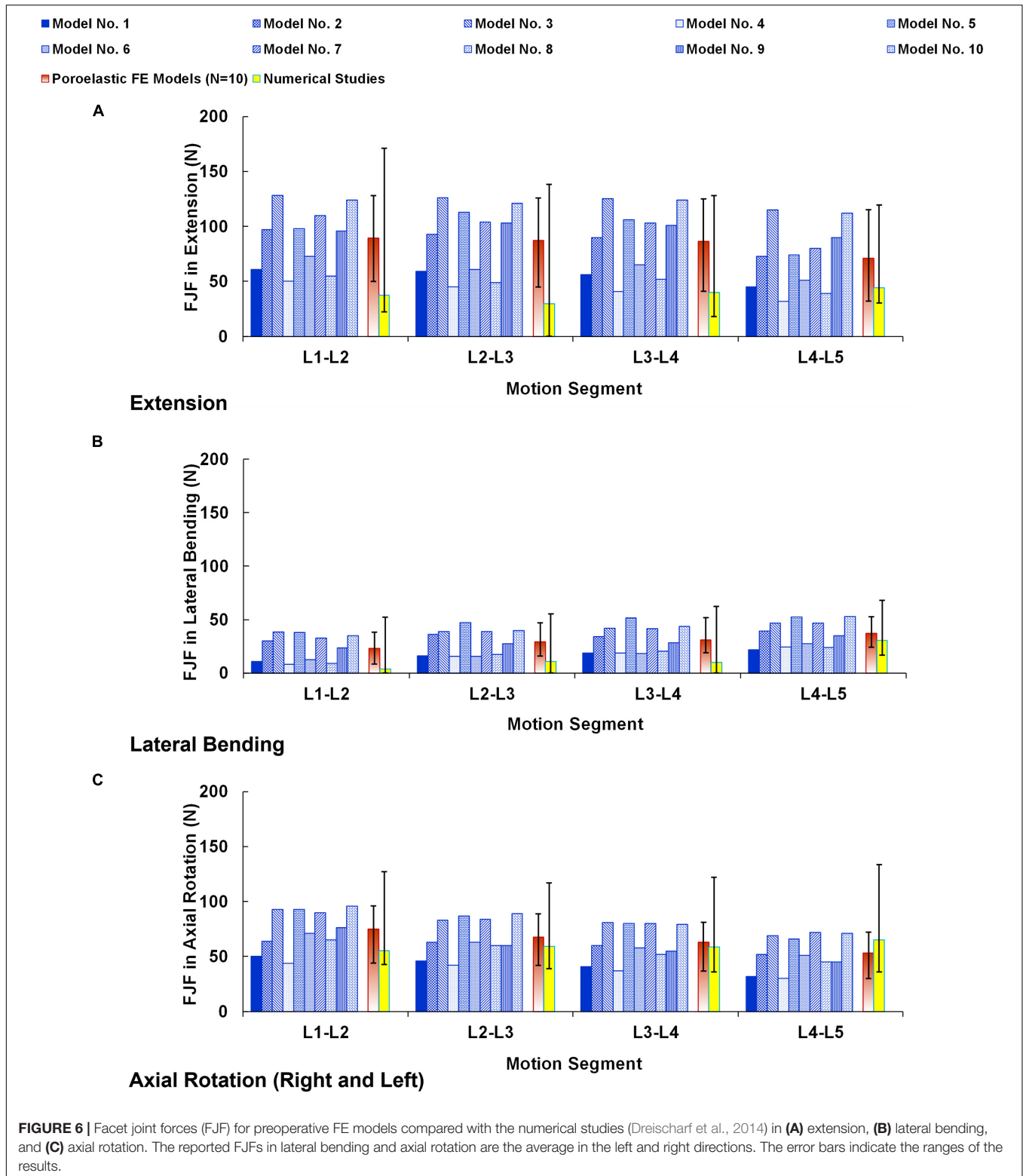
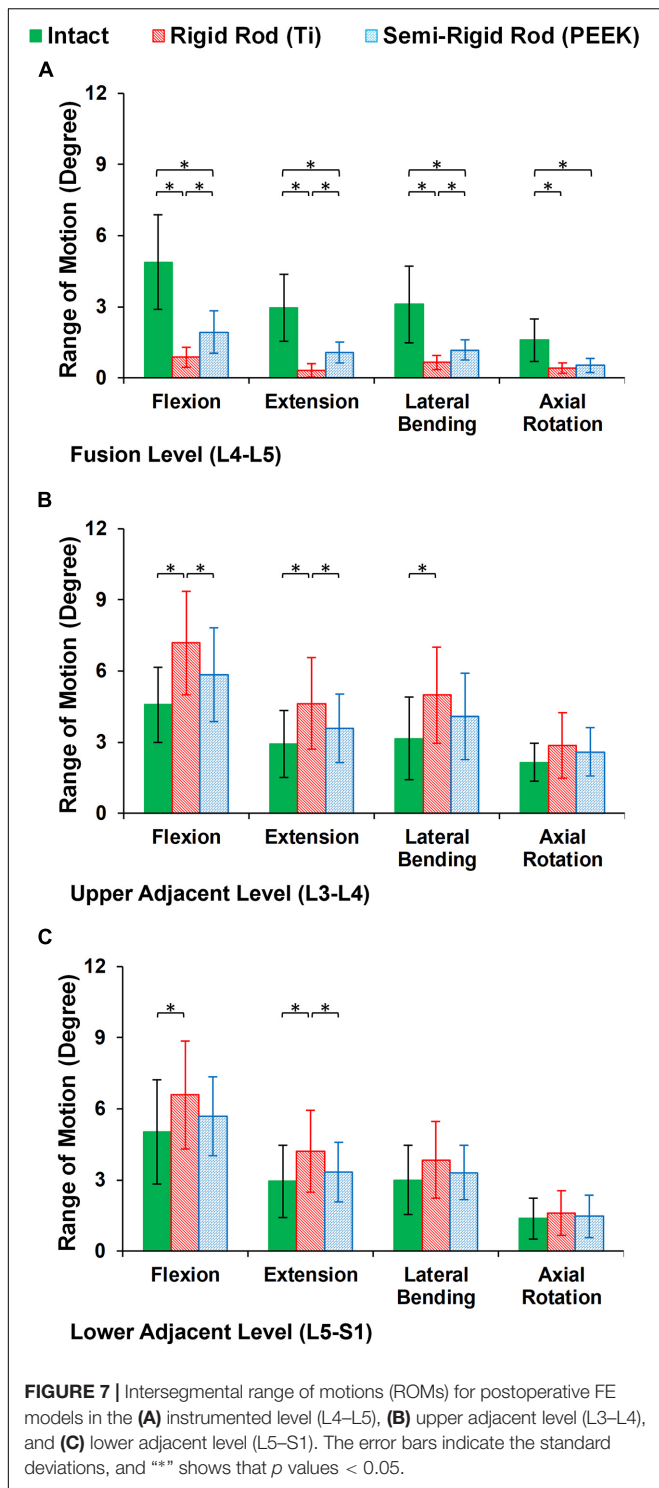


FIGURE 5 | Intradiscal pressure (IDP) for preoperative FE models compared with the numerical studies (Dreischarf et al., 2014) in **(A)** flexion, **(B)** extension, **(C)** lateral bending, and **(D)** axial rotation. The reported IDPs in lateral bending and axial rotation are the average in the left and right directions. The error bars indicate the ranges of the results.



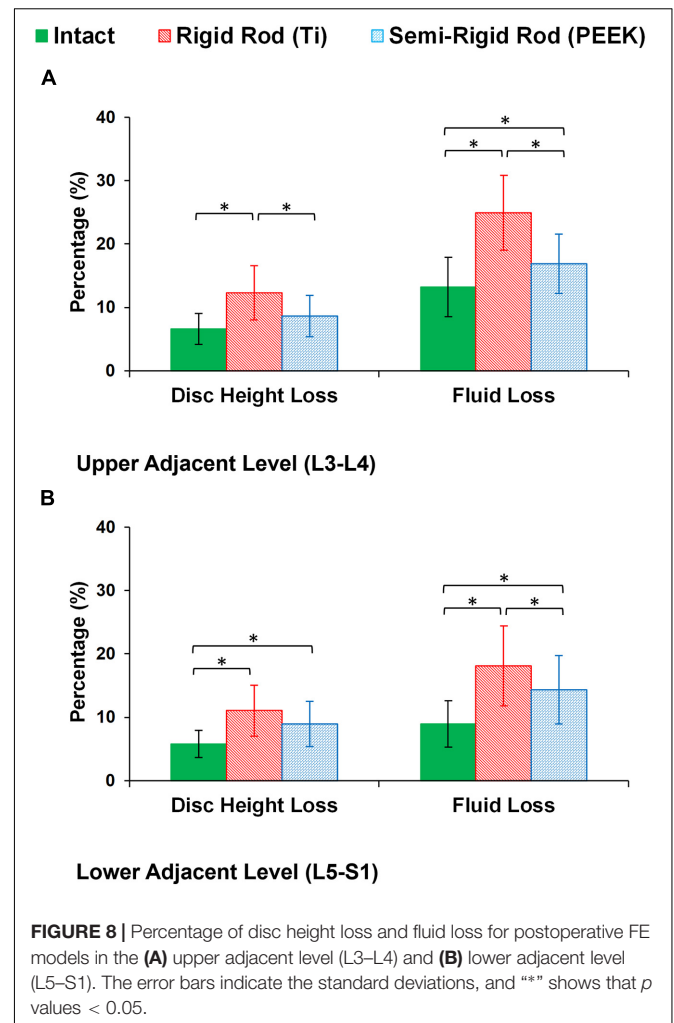
differences among patients may cause indecision in the results and decrease the reliability of the FE model prediction. This study provided a validated parametric poroelastic FE model to evaluate the results for different patients and provide more

accurate clinical outcome. Although the clinical applicability of this FE modeling technique was previously confirmed, the attained results from these 10 preop poroelastic models (i.e., ROM, IDP, and FJF) were generally in alignment with previous



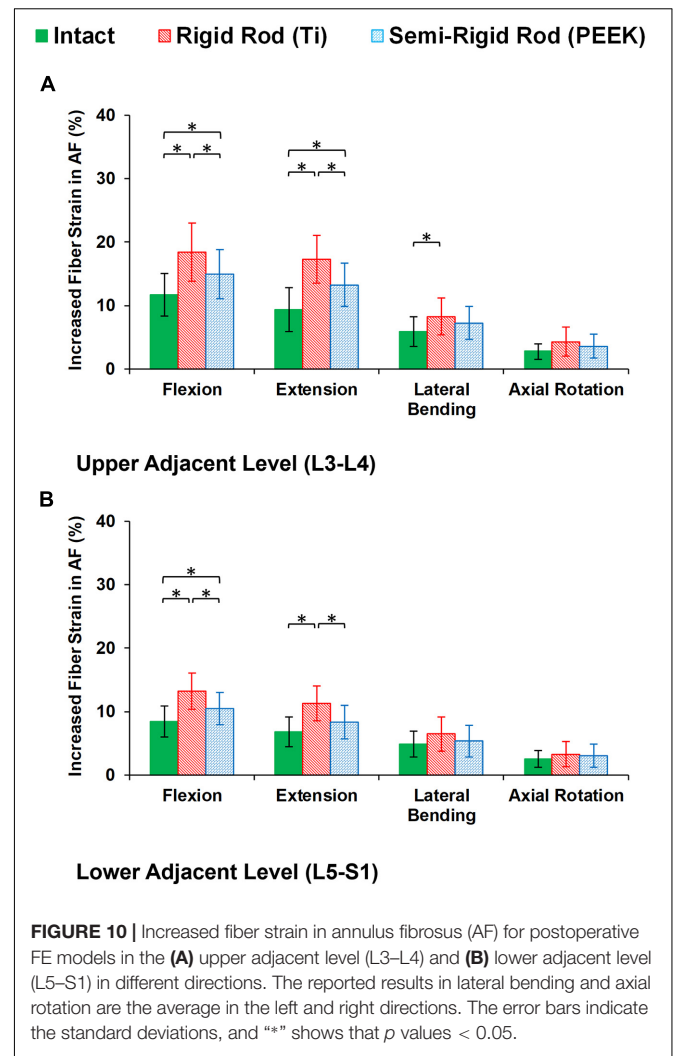
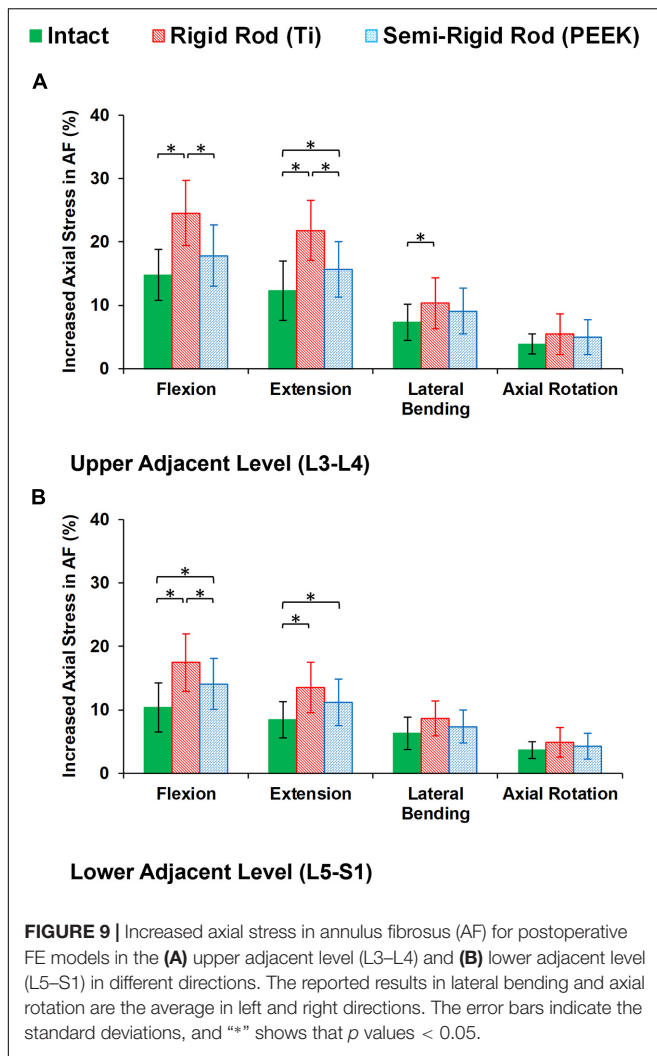
published studies (Dreischarf et al., 2014) confirming the validity of these models. The mechanical responses achieved by different models (Figures 4–6) confirm the important influences of the geometry and curvature of the lumbar spine.

The postop simulations showed that the average ROM significantly decreased for both Ti and PEEK rod constructs at



the instrumented level (L4–L5) in all directions. As expected, the ROM in the instrumented level was significantly higher in the PEEK models compared with Ti ones based on its structural flexibility. Increased ROMs at adjacent levels (L3–L4 and L5–S1) were observed for the Ti rod group compared with the intact and PEEK rod group which may indicate the risk of disc degeneration in adjacent levels for rigid fixation. Minor alterations in adjacent level ROM were observed in lateral bending, and the differences in axial rotation were not significant. Similar to the aforementioned pattern, disc height loss and fluid loss were significantly higher at adjacent levels in the Ti rod group after 16 h of cycling loading during daily activities, which alter the fluid–solid interaction of the adjacent IVDs.

Disc height loss is an important clinical indicator for disc degeneration. The loss of disc height across all levels of the prep FE models was approximately uniform but was altered in the postop models. The rigidity of the Ti rod system in the L4–L5 level subsequently increased the load sharing through the adjacent levels revealing a significant increase in disc height loss and fluid loss. Previous clinical studies reported IVD height loss in adjacent levels for 30–95% of the patients who had fusion



surgery utilizing Ti rods (Miyakoshi et al., 2000; Ishihara et al., 2001). Consistent with previous clinical (Huang et al., 2016) and *in vitro* (Turner et al., 2010; Gornet et al., 2011; Chou et al., 2015) studies, the PEEK construct preserved part of the ROM at the fused level and reduced the abnormal compensatory load sharing at the adjacent levels. Similar patterns were observed regarding fluid loss in adjacent IVDs in postop FE models. Fluid loss debilitates the damping quality, which results in disc disability in absorbing stress. Such finding may suggest the advantage of using a semirigid fixation system to decrease the chance of ASD. The achieved standard deviations in the reported results show considerable ranges for the altered mechanical responses after surgery in different patients, which highlights the importance of interanatomical variability in clinical evaluations.

The findings of this study also confirmed that stress and fiber strain in the AF region were significantly increased in adjacent levels for the fused model in sagittal plane movements (i.e., flexion and extension). Besides, the increased stress and strain were significantly higher in rigid Ti fixation compared with the semirigid PEEK rod. The PEEK rod system transfers more of the

compressive load from the posterior column to the anterior side. This demonstrates the ability to change the stress distribution and improve the conditions similar to the intact lumbar spine. After repetitive cyclic loading, greater fluid loss and disc height loss were observed in the rigid construct, which results in decreasing the effect of fluid phase in overall bulk strength that may lead to more experienced stress and strain in the solid phase. The ROM, fluid flow, and load sharing results are in general agreement with those presented in previous studies (Gornet et al., 2011; Chou et al., 2015; Huang et al., 2016) confirming the potential advantages of PEEK over Ti fixation.

Few simplifications were assumed for this study. First, the geometry of the patient-specific FE models was constructed based on simplified structures on X-ray images, and the same material properties were used for all different individuals in this study. In addition, more simplifications were considered regarding the poroelastic FE modeling of the IVD compared with some previous works in the literature (Castro et al., 2014; Barthelemy et al., 2016; Rijsbergen et al., 2018; Castro and Alves, 2020). As discussed in detail in a previous work (Nikkhoo et al., 2020),

this parametric patient-specific FE modeling technique can accurately predict the biomechanical response of the lumbar spine in association with various surgical interventions and has the potential to be used in clinical evaluations. As we focused on clinical functionality of this modeling technique, the variation in mechanical properties for different patients was neglected, although it remains a potential framework for our future works. Second, we used the osseoligamentous FE models for this study and the effect of active muscle forces was ignored. Since the objective of this study was to evaluate the effect of posterolateral fixation surgery using rigid and semirigid rods on lumbar spine biomechanics, we applied the common follower load technique (Patwardhan et al., 1999; Shirazi-Adl and Parnianpour, 2000) to account for compressive loading regime for both static and simulated daily activities. Nevertheless, although the current osseoligamentous FE model compensates for the global response for this study, enhancing the model by inserting muscle force effects may improve the model assumptions, especially if we can extract the patient-specific muscle forces *via* dynamic algorithms. Third, we considered the fully saturated porous media in FE model calculations which is a simplification for the patients' IVDs which may be denatured or degenerated. When we calculate the fluid flow and consequently investigate disc height changes and fluid loss, it is important to have accurate data for initial void ratio and fluid saturation rate. This was an unavoidable limitation in this study, and we assumed constant conditions (i.e., similar void ratios based on **Table 1** and fully saturated porous media) for all patients. On the other hand, we mimicked the posterolateral fixation surgery in the L4–L5 level and its IVD was intact in the simulations. To check the influence of mild and moderate degeneration in L4–L5 IVD, extra calculations were performed for three models using altered material properties (Galbusera et al., 2011a), and no significant changes were observed for the variations of the stress and strain patterns in adjacent levels. As we compared the three scenarios for each patient, the achieved results can be reliable for an overall comparison and this limitation may be tolerated.

CONCLUSION

This study presents a validated geometrically patient-specific poroelastic FE modeling technique, which has the potential to be utilized for clinical applications to analyze lumbar spine biomechanics. This FE model was applied to investigate the effect of posterolateral fixation surgery on the biomechanics of the adjacent levels, and rigid (Ti) versus semirigid (PEEK) rod fixation systems were compared. The results indicated that

REFERENCES

- Argoubi, M., and Shirazi-Adl, A. (1996). Poroelastic creep response analysis of a lumbar motion segment in compression. *J. Biomech.* 29, 1331–1339. doi: 10.1016/0021-9290(96)00035-8
- Aygün, H., Çakar, A., Hüseyinoğlu, N., Hüseyinoğlu, U., and Çelik, R. (2014). Clinical and radiological comparison of posterolateral fusion and posterior interbody fusion techniques for multilevel lumbar spinal stabilization in manual workers. *Asian Spine J.* 8:571. doi: 10.4184/asj.2014.8.5.571
- Barthelemy, V. M. P., van Rijsbergen, M. M., Wilson, W., Huyghe, J. M., van Rietbergen, B., and Ito, K. (2016). A computational spinal motion segment model incorporating a matrix composition-based model of the intervertebral disc. *J. Mech. Behav. Biomed. Mater.* 54, 194–204. doi: 10.1016/j.jmbm.2015.09.028
- Bashkuev, M., Reitmaier, S., and Schmidt, H. (2018). Effect of disc degeneration on the mechanical behavior of the human lumbar spine: a probabilistic finite element study. *Spine J.* 18, 1910–1920. doi: 10.1016/j.spinee.2018.05.046

increased ROM, experienced stress in AF, and fiber strain at adjacent levels were observed for the Ti rod compared with the intact and PEEK rod, which may progress the risk of disc degeneration in adjacent levels for rigid fixation. Similarly, disc height loss and fluid loss were significantly higher at adjacent levels in the Ti rod group after daily cycling loading which alter the fluid–solid interaction of the discs and can be an important clinical indicator for degeneration. In summary, this study confirms the differences in the poroelastic characteristics of adjacent discs for semirigid (PEEK) and rigid (Ti) constructs and reveals the advantage of PEEK for decreasing the risk of ASD.

DATA AVAILABILITY STATEMENT

The raw data supporting the conclusions of this article will be made available by the authors, without undue reservation.

ETHICS STATEMENT

Written informed consent was obtained from the individual(s) for the publication of any potentially identifiable images or data included in this article.

AUTHOR CONTRIBUTIONS

All authors listed above have made substantial contributions to the conception and design of the study, analysis and interpretation of data, preparing the manuscript, and also attest to the validity and legitimacy of the data and its interpretation, and approved it for publication.

FUNDING

The authors thank the Chang Gung Memorial Hospital Research Program (CRRPG3H0062 and CMRPD1J0152), the Healthy Aging Research Center, Chang Gung University, Taiwan (EMRPD1L0411), and the Ministry of Science and Technology of the Republic of China (107-2221-E-182-018-MY3 to C-HC) for scientific funding and support.

ACKNOWLEDGMENTS

The authors appreciate Mrs. Zahra Khoz's help during this study.

- Beatty, S. (2018). We need to talk about lumbar total disc replacement. *Int. J. Spine Surg.* 12, 201–240. doi: 10.14444/5029
- Campbell, R. C., Mobbs, R. J., Lu, V. M., Xu, J., Rao, P. J., and Phan, K. (2017). Posterolateral fusion versus interbody fusion for degenerative spondylolisthesis: systematic review and meta-analysis. *Glob. Spine J.* 7, 482–490. doi: 10.1177/2192568217701103
- Castro, A. P. G., and Alves, J. L. (2020). Numerical implementation of an osmoporo-visco-hyperelastic finite element solver: application to the intervertebral disc. *Comput. Methods Biomech. Biomed. Eng.* (in press):1–13. doi: 10.1080/10255842.2020.1839059
- Castro, A. P. G., Wilson, W., Huyghe, J. M., Ito, K., and Alves, J. L. (2014). Intervertebral disc creep behavior assessment through an open source finite element solver. *J. Biomech.* 47, 297–301. doi: 10.1016/j.jbiomech.2013.10.014
- Castro, A. P. G., Yao, J., Battisti, T., and Lacroix, D. (2018). Poroelastic modeling of highly hydrated collagen hydrogels: experimental results vs. numerical simulation with custom and commercial finite element solvers. *Front. Bioeng. Biotechnol.* 6:142. doi: 10.3389/fbioe.2018.00142
- Chiang, M.-F., Zhong, Z.-C., Chen, C.-S., Cheng, C.-K., and Shih, S.-L. (2006). Biomechanical comparison of instrumented posterior lumbar interbody fusion with one or two cages by finite element analysis. *Spine* 31, E682–E689. doi: 10.1097/01.brs.0000232714.72699.8e
- Chou, W.-K., Chien, A., and Wang, J.-L. (2015). Biomechanical analysis between PEEK and titanium screw-rods spinal construct subjected to fatigue loading. *J. Spine. Disord. Techn.* 28, E121–E125. doi: 10.1097/bsd.0000000000000176
- De Iure, F., Bosco, G., Cappuccio, M., Paderni, S., and Amendola, L. (2012). Posterior lumbar fusion by peek rods in degenerative spine: preliminary report on 30 cases. *Eur. Spine J.* 21(Suppl. 1), S50–S54. doi: 10.1007/s00586-012-2219-x
- Dreischarf, M., Rohlmann, A., Bergmann, G., and Zander, T. (2011). Optimised loads for the simulation of axial rotation in the lumbar spine. *J. Biomech.* 44, 2323–2327. doi: 10.1016/j.jbiomech.2011.05.040
- Dreischarf, M., Rohlmann, A., Bergmann, G., and Zander, T. (2012). Optimised in vitro applicable loads for the simulation of lateral bending in the lumbar spine. *Med. Eng. Phys.* 34, 777–780. doi: 10.1016/j.medengphys.2012.04.002
- Dreischarf, M., Zander, T., Shirazi-Adl, A., Puttlitz, C. M., Adam, C. J., Chen, C. S., et al. (2014). Comparison of eight published static finite element models of the intact lumbar spine: predictive power of models improves when combined together. *J. Biomech.* 47, 1757–1766. doi: 10.1016/j.jbiomech.2014.04.002
- El-Rich, M., Arnoux, P. J., Wagnac, E., Brunet, C., and Aubin, C. E. (2009). Finite element investigation of the loading rate effect on the spinal load-sharing changes under impact conditions. *J. Biomech.* 42, 1252–1262. doi: 10.1016/j.jbiomech.2009.03.036
- Ferguson, S. J., Ito, K., and Nolte, L.-P. (2004). Fluid flow and convective transport of solutes within the intervertebral disc. *J. Biomech.* 37, 213–221. doi: 10.1016/s0021-9290(03)00250-1
- Galbusera, F., Schmidt, H., Neidlinger-Wilke, C., and Wilke, H.-J. (2011a). The effect of degenerative morphological changes of the intervertebral disc on the lumbar spine biomechanics: a poroelastic finite element investigation. *Comput. Methods Biomech. Biomed. Eng.* 14, 729–739. doi: 10.1080/10255842.2010.493522
- Galbusera, F., Schmidt, H., Noailly, J., Malandrino, A., Lacroix, D., Wilke, H.-J., et al. (2011b). Comparison of four methods to simulate swelling in poroelastic finite element models of intervertebral discs. *J. Mech. Behav. Biomed. Mater.* 4, 1234–1241. doi: 10.1016/j.jmbm.2011.04.008
- Ghobadiha, E., Nikkhoo, M., and Naserkhaki, S. (2019). Poroelastic finite element modeling of a lumbar spine motion segment and validation in different motions for clinical studies. *Iran. J. Orthopaed. Surg.* 17, 142–152.
- Gornet, M. F., Chan, F. W., Coleman, J. C., Murrell, B., Nockels, R. P., Taylor, B. A., et al. (2011). Biomechanical assessment of a PEEK rod system for semi-rigid fixation of lumbar fusion constructs. *J. Biomech. Eng.* 133:081009. doi: 10.1115/1.4004862
- Goto, K., Tajima, N., Chosa, E., Totoribe, K., Kubo, S., Kuroki, H., et al. (2003). Effects of lumbar spinal fusion on the other lumbar intervertebral levels (three-dimensional finite element analysis). *J. Orthop. Sci.* 8, 577–584. doi: 10.1007/s00776-003-0675-1
- Guo, T.-M., Lu, J., Xing, Y.-L., Liu, G.-X., Zhu, H.-Y., Yang, L., et al. (2019). A 3-dimensional finite element analysis of adjacent segment disk degeneration induced by transforaminal lumbar interbody fusion after pedicle screw fixation. *World Neurosurg.* 124, e51–e57. doi: 10.1016/j.wneu.2018.11.195
- Heo, M., Yun, J., Park, S. H., Choi, Y. S., Lee, S. S., and Park, S. (2020). Design of a lumbar interspinous fixation device for minimally invasive surgery and spine motion stabilization. *J. Med. Biol. Eng.* 40, 1–10. doi: 10.1007/s40846-019-00485-8
- Highsmith, J. M., Tumlalán, L. M., and Rodts, G. E. (2007). Flexible rods and the case for dynamic stabilization. *Neurosurg. Focus* 22, 1–5. doi: 10.3171/foc.2007.22.1.11
- Huang, W., Chang, Z., Song, R., Zhou, K., and Yu, X. (2016). Non-fusion procedure using PEEK rod systems for lumbar degenerative diseases: clinical experience with a 2-year follow-up. *BMC Musculosk. Disord.* 17:53. doi: 10.1186/s12891-016-0913-2
- Iatridis, J. C., Laible, J. P., and Krag, M. H. (2003). Influence of fixed charge density magnitude and distribution on the intervertebral disc: applications of a Poroelastic and Chemical Electric (PEACE) model. *J. Biomech. Eng.* 125, 12–24. doi: 10.1115/1.1537190
- Ishihara, H., Osada, R., Kanamori, M., Kawaguchi, Y., Ohmori, K., Kimura, T., et al. (2001). Minimum 10-Year follow-up study of anterior lumbar interbody fusion for isthmic spondylolisthesis. *J. Spine. Disord.* 14, 91–99. doi: 10.1097/00002517-200104000-00001
- Jahng, T.-A., Kim, Y. E., and Moon, K. Y. (2013). Comparison of the biomechanical effect of pedicle-based dynamic stabilization: a study using finite element analysis. *Spine J.* 13, 85–94. doi: 10.1016/j.spinee.2012.11.014
- Jin, Y. J., Kim, Y. E., Seo, J. H., Choi, H. W., and Jahng, T.-A. (2012). Effects of rod stiffness and fusion mass on the adjacent segments after floating monosegmental fusion: a study using finite element analysis. *Eur. Spine J.* 22, 1066–1077. doi: 10.1007/s00586-012-2611-6
- Laville, A., Laporte, S., and Skalli, W. (2009). Parametric and subject-specific finite element modelling of the lower cervical spine. Influence of geometrical parameters on the motion patterns. *J. Biomech.* 42, 1409–1415. doi: 10.1016/j.jbiomech.2009.04.007
- Lee, J. C., Kim, Y., Soh, J.-W., and Shin, B.-J. (2014). Risk factors of adjacent segment disease requiring surgery after lumbar spinal fusion. *Spine* 39, E339–E345. doi: 10.1097/brs.0000000000000164
- Li, C., Liu, L., Shi, J.-Y., Yan, K.-Z., Shen, W.-Z., and Yang, Z.-R. (2016). Clinical and biomechanical researches of polyetheretherketone (PEEK) rods for semi-rigid lumbar fusion: a systematic review. *Neurosurg. Rev.* 41, 375–389. doi: 10.1007/s10143-016-0763-2
- Lidar, Z., Beaumont, A., Lifshutz, J., and Maiman, D. J. (2005). Clinical and radiological relationship between posterior lumbar interbody fusion and posterolateral lumbar fusion. *Surg. Neurol.* 64, 303–308. doi: 10.1016/j.surneu.2005.03.025
- Liu, M. Y., Tsai, T. T., Chen, L. H., Liang, W. H., Lai, P. L., and Tai, C. L. (2020). Biomechanical comparison of lumbar motion unit stability following posterior instrumentation with facet spacers and facet screws. *J. Med. Biol. Eng.* 40, 220–229. doi: 10.1007/s40846-019-00501-x
- Miyakoshi, N., Abe, E., Shimada, Y., Okuyama, K., Suzuki, T., and Sato, K. (2000). Outcome of One-level posterior lumbar interbody fusion for spondylolisthesis and postoperative intervertebral disc degeneration adjacent to the fusion. *Spine* 25, 1837–1842. doi: 10.1097/00007632-200007150-00016
- Naserkhaki, S., and El-Rich, M. (2017). Sensitivity of lumbar spine response to follower load and flexion moment: finite element study. *Comput. Methods Biomech. Biomed. Engin.* 20, 550–557. doi: 10.1080/10255842.2016.1257707
- Naserkhaki, S., Jaremko, J. L., Adeeb, S., and El-Rich, M. (2016). On the load-sharing along the ligamentous lumbosacral spine in flexed and extended postures: finite element study. *J. Biomech.* 49, 974–982. doi: 10.1016/j.jbiomech.2015.09.050
- Nikitovic, D., Más, Y., Gracia, L., Ibarz, E., Gabarre, S., Peña, D., et al. (2017). Finite element simulation and clinical follow-up of lumbar spine biomechanics with dynamic fixations. *PLoS One* 12:e0188328. doi: 10.1371/journal.pone.0188328
- Nikkhoo, M., Cheng, C. H., Wang, J. L., Khoz, Z., El-Rich, M., Hebel, N., et al. (2019). Development and validation of a geometrically personalized finite element model of the lower ligamentous cervical spine for clinical applications. *Comput. Biol. Med.* 109, 22–32. doi: 10.1016/j.combiomed.2019.04.010
- Nikkhoo, M., Haghpanahi, M., Parnianpour, M., and Wang, J.-L. (2013a). Dynamic responses of intervertebral disc during static creep and dynamic cyclic loading:

- a parametric poroelastic finite element analysis. *Biomed. Eng. Appl. Basis Commun.* 25:1350013.
- Nikkhoo, M., Hsu, Y.-C., Haghpanahi, M., Parnianpour, M., and Wang, J.-L. (2013b). A meta-model analysis of a finite element simulation for defining poroelastic properties of intervertebral discs. *Proc. Instit. Mech. Eng. Part H* 227, 672–682.
- Nikkhoo, M., Khoz, Z., Cheng, C.-H., Niu, C.-C., El-Rich, M., and Khalaf, K. (2020). Development of a novel geometrically-parametric patient-specific finite element model to investigate the effects of the lumbar lordosis angle on fusion surgery. *J. Biomech.* 102:109722. doi: 10.1016/j.jbiomech.2020.109722
- Ormond, D. R., Albert, L. Jr., and Das, K. (2016). Polyetheretherketone (PEEK) rods in lumbar spine degenerative disease: a case series. *Clin. Spine Surg.* 29, E371–E375. doi: 10.1097/BSD.0b013e318277cb9b
- Ozkal, F. M., Cakir, F., and Sensoz, E. (2020). Schematization of cannulated screw fixations in femoral neck fractures using genetic algorithm and finite element method. *J. Med. Biol. Eng.* 40, 673–687. doi: 10.1007/s40846-020-00528-5
- Park, W. M., Kim, K., and Kim, Y. H. (2013). Effects of degenerated intervertebral discs on intersegmental rotations, intradiscal pressures, and facet joint forces of the whole lumbar spine. *Comput. Biol. Med.* 43, 1234–1240. doi: 10.1016/j.compbimed.2013.06.011
- Patwardhan, A. G., Havey, R. M., Meade, K. P., Lee, B., and Dunlap, B. (1999). A follower load increases the load-carrying capacity of the lumbar spine in compression. *Spine* 24, 1003–1009. doi: 10.1097/00007632-199905150-00014
- Pintar, F. A., Yoganandan, N., Myers, T., Elhagediab, A., and Sances, A. (1992). Biomechanical properties of human lumbar spine ligaments. *J. Biomech.* 25, 1351–1356. doi: 10.1016/0021-9290(92)90290-h
- Rahm, M. D., and Hall, B. B. (1996). Adjacent-segment degeneration after lumbar fusion with instrumentation: a retrospective study. *J. Spinal Disord.* 9, 392–400.
- Rijsbergen, M. V., Rietbergen, B. V., Barthelemy, V., Eltes, P., Lazáry, Á, Lacroix, D., et al. (2018). Comparison of patient-specific computational models vs. clinical follow-up, for adjacent segment disc degeneration and bone remodelling after spinal fusion. *PLoS One* 13:e0200899. doi: 10.1371/journal.pone.0200899
- Rohlmann, A., Zander, T., Rao, M., and Bergmann, G. (2009). Realistic loading conditions for upper body bending. *J. Biomech.* 42, 884–890. doi: 10.1016/j.jbiomech.2009.01.017
- Schmidt, H., Galbusera, F., Rohlmann, A., and Shirazi-Adl, A. (2013). What have we learned from finite element model studies of lumbar intervertebral discs in the past four decades? *J. Biomech.* 46, 2342–2355. doi: 10.1016/j.jbiomech.2013.07.014
- Schmidt, H., Heuer, F., Simon, U., Kettler, A., Rohlmann, A., Claes, L., et al. (2006). Application of a new calibration method for a three-dimensional finite element model of a human lumbar annulus fibrosus. *Clin. Biomech.* 21, 337–344. doi: 10.1016/j.clinbiomech.2005.12.001
- Schmidt, H., Kettler, A., Heuer, F., Simon, U., Claes, L., and Wilke, H. J. (2007a). Intradiscal pressure, shear strain, and fiber strain in the intervertebral disc under combined loading. *Spine* 32, 748–755. doi: 10.1097/01.brs.0000259059.90430.c2
- Schmidt, H., Kettler, A., Rohlmann, A., Claes, L., and Wilke, H. J. (2007b). The risk of disc prolapses with complex loading in different degrees of disc degeneration - a finite element analysis. *Clin. Biomech.* 22, 988–998. doi: 10.1016/j.clinbiomech.2007.07.008
- Schmidt, H., Shirazi-Adl, A., Galbusera, F., and Wilke, H. J. (2010). Response analysis of the lumbar spine during regular daily activities—a finite element analysis. *J. Biomech.* 43, 1849–1856. doi: 10.1016/j.jbiomech.2010.03.035
- Schroeder, Y., Huyghe, J. M., van Donkelaar, C. C., and Ito, K. (2010). A biochemical/biophysical 3D FE intervertebral disc model. *Biomech. Model. Mechanobiol.* 9, 641–650. doi: 10.1007/s10237-010-0203-0
- Schwab, F. J., Nazarian, D. G., Mahmud, F., and Michelsen, C. B. (1995). Effects of spinal instrumentation on fusion of the lumbosacral spine. *Spine* 20, 2023–2028. doi: 10.1097/00007632-199509150-00014
- Selim, A., Mercer, S., and Tang, F. (2018). Polyetheretherketone (PEEK) rods for lumbar fusion: a systematic review and meta-analysis. *Intern. J. Spine Surg.* 12, 190–200. doi: 10.14444/5027
- Serhan, H., Mhatre, D., Defossez, H., and Bono, C. M. (2011). Motion-preserving technologies for degenerative lumbar spine: the past, present, and future horizons. *SAS J.* 5, 75–89. doi: 10.1016/j.esas.2011.05.001
- Shih, S. L., Liu, C. L., Huang, L. Y., Huang, C. H., and Chen, C. S. (2013). Effects of cord pretension and stiffness of the Dynesys system spacer on the biomechanics of spinal decompression- a finite element study. *BMC Musculoskelet. Disord.* 14:191. doi: 10.1186/1471-2474-14-191
- Shirazi-Adl, A., Ahmed, A. M., and Shrivastava, S. C. (1986a). A finite element study of a lumbar motion segment subjected to pure sagittal plane moments. *J. Biomech.* 19, 331–350. doi: 10.1016/0021-9290(86)90009-6
- Shirazi-Adl, A., Ahmed, A. M., and Shrivastava, S. C. (1986b). Mechanical response of a lumbar motion segment in axial torque alone and combined with compression. *Spine* 11, 914–927.
- Shirazi-Adl, A., and Parnianpour, M. (2000). Load-bearing and stress analysis of the human spine under a novel wrapping compression loading. *Clin. Biomech.* 15, 718–725. doi: 10.1016/s0268-0033(00)00045-0
- Simon, B. R. (1992). Multiphase poroelastic finite element models for soft tissue structures. *Appl. Mech. Rev.* 45, 191–218. doi: 10.1115/1.3121397
- Sudo, H., Oda, I., Abumi, K., Ito, M., Kotani, Y., and Minami, A. (2006). Biomechanical study on the effect of five different lumbar reconstruction techniques on adjacent-level intradiscal pressure and lamina strain. *J. Neurosurg.* 5, 150–155. doi: 10.3171/spi.2006.5.2.150
- Turner, J. L., Paller, D. J., and Murrell, C. B. (2010). The mechanical effect of commercially pure titanium and polyetheretherketone rods on spinal implants at the operative and adjacent levels. *Spine* 35, E1076–E1082. doi: 10.1097/BRS.0b013e3181d1fb85
- Wang, H., Ma, L., Yang, D., Wang, T., Liu, S., Yang, S., et al. (2017). Incidence and risk factors of adjacent segment disease following posterior decompression and instrumented fusion for degenerative lumbar disorders. *Medicine* 96:e6032. doi: 10.1097/MD.00000000000006032
- Zhang, Z., Fogel, G. R., Liao, Z., Sun, Y., and Liu, W. (2018a). Biomechanical analysis of lumbar interbody fusion cages with various lordotic angles: a finite element study. *Comput. Methods Biomech. Biomed. Engin.* 21, 247–254. doi: 10.1080/10255842.2018.1442443
- Zhang, Z., Li, H., Fogel, G. R., Liao, Z., Li, Y., and Liu, W. (2018b). Biomechanical analysis of porous additive manufactured cages for lateral lumbar interbody fusion: a finite element analysis. *World Neurosurg.* 111, e581–e591. doi: 10.1016/j.wneu.2017.12.127

Conflict of Interest: The authors declare that the research was conducted in the absence of any commercial or financial relationships that could be construed as a potential conflict of interest.

Copyright © 2021 Nikkhoo, Lu, Chen, Fu, Niu, Lin and Cheng. This is an open-access article distributed under the terms of the Creative Commons Attribution License (CC BY). The use, distribution or reproduction in other forums is permitted, provided the original author(s) and the copyright owner(s) are credited and that the original publication in this journal is cited, in accordance with accepted academic practice. No use, distribution or reproduction is permitted which does not comply with these terms.